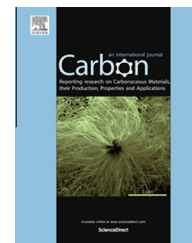


Available at [www.sciencedirect.com](http://www.sciencedirect.com)

ScienceDirect

journal homepage: [www.elsevier.com/locate/carbon](http://www.elsevier.com/locate/carbon)

# Influence of lattice orientation on growth and structure of graphene on Cu(001)



Joseph M. Wofford <sup>a,\*</sup>, Shu Nie <sup>b</sup>, Konrad Thürmer <sup>b</sup>, Kevin F. McCarty <sup>b</sup>,  
Oscar D. Dubon <sup>a,\*</sup>

<sup>a</sup> Department of Materials Science & Engineering, University of California at Berkeley, and Lawrence Berkeley National Laboratory, Berkeley, CA 94720, USA

<sup>b</sup> Sandia National Laboratories, Livermore, CA 94550, USA

## ARTICLE INFO

### Article history:

Received 11 November 2014

Accepted 23 March 2015

Available online 31 March 2015

## ABSTRACT

We have used low-energy electron microscopy (LEEM) and diffraction (LEED) to examine the significance of lattice orientation in graphene growth on Cu(001). Individual graphene domains undergo anisotropic growth on the Cu surface, and develop into lens shapes with their long axes roughly aligned with Cu(100) in-plane directions. The long axis of a lens-shaped domain is only rarely oriented along a C(11) direction, suggesting that carbon attachment at “zigzag” graphene island edges is unfavorable. A kink-mediated adatom attachment process is consistent with the behavior observed here and reported in the literature. The details of the ridged moiré pattern formed by the superposition of the graphene lattice on the (001) Cu surface also evolve with the graphene lattice orientation, and are predicted well by a simple geometric model. Managing the kink-mediated growth mode of graphene on Cu(001) will be necessary for the continued improvement of this graphene synthesis technique.

© 2015 Elsevier Ltd. All rights reserved.

## 1. Introduction

Copper foils have proven to be an effective substrate for graphene growth. The (001)-textured Cu foils support the growth of large-area polycrystalline graphene films, which none-the-less remain exclusively one monolayer thick due to the low solubility of C in the metal [1–4]. Recent refinement of this growth process has yielded individual graphene islands exceeding 1 mm in size [5,6]. The scientific and technological significance of these results has made characterizing the fundamental processes behind this synthesis technique an urgent priority.

The microstructure of a thin film, or its “quality”, is typically determined during its growth. Films with low defect densities usually have an epitaxial relationship with the crystalline substrate. The extent to which epitaxy is achieved depends on the crystal structures of both the film and the substrate. Thus, understanding the relationship between the combined film-substrate crystallography and growth behavior is a prerequisite to systematically improve film quality. Here the crystallography of the graphene/Cu(001) system is defined by the 6-fold symmetric graphene lattice, the 4-fold symmetric surface of the Cu facet, and the relative in-plane orientation of the two lattices. The

\* Corresponding authors: Current Address: Paul-Drude-Institut für Festkörperelektronik, Hausvogteiplatz 5-7, 10117 Berlin, Germany (J.M. Wofford).

E-mail addresses: [joewofford@gmail.com](mailto:joewofford@gmail.com) (J.M. Wofford), [oddubon@berkeley.edu](mailto:oddubon@berkeley.edu) (O.D. Dubon).

<http://dx.doi.org/10.1016/j.carbon.2015.03.056>

0008-6223/© 2015 Elsevier Ltd. All rights reserved.

graphene and Cu lattices are perfectly aligned when a  $C\langle 10 \rangle$  direction is parallel to one of two equivalent in-plane orientations,  $Cu[110]$  or  $Cu[\bar{1}\bar{1}0]$ . However, the lattices of most graphene domains are rotated some degrees away from such ideal alignment, resulting in a range of different graphene configurations on the Cu surface [4].

A straightforward examination of the symmetry of the graphene/Cu(001) system begins to reveal how the interplay between crystallography and growth behavior unfolds. The symmetry of the combined structure is determined by which symmetry elements are common to the graphene lattice and Cu surface: a 2-fold rotation. This 2-fold axis is manifested in the moiré formed by the superposition of the hexagonal graphene lattice on the (001) surface of the Cu. Rather than forming a hexagonal superlattice as graphene does on a close-packed metal facet [7–11], here the moiré gives rise to a periodic array of parallel ridges in the graphene [12–14]. The combined graphene–Cu(001) symmetry is also reflected in the shape evolution of individual graphene crystals growing on the Cu, where a 2-fold symmetric anisotropic growth rate sculpts many graphene crystals into elongated, lens-like profiles (for an extended discussion please see Ref. [4]). The long axes of the lens-shaped graphene crystals – which we define as their “fast growth direction” – align roughly with the  $Cu\langle 100 \rangle$  in-plane directions, illustrating explicitly the influence of the substrate crystallography.

While this symmetry analysis is useful as a phenomenological guide, it neglects many details of the growth process. An exhaustive study that includes the relative in-plane orientation of the graphene lattice is necessary to fully understand the significance of crystallography in this growth system. Here low-energy electron microscopy (LEEM) and diffraction (LEED) were used to study graphene growth by molecular beam epitaxy (MBE). In particular, we examined the influence of the graphene lattice orientation on its fast growth direction and moiré pattern.

## 2. Experimental methods

Graphene films were synthesized on 25- $\mu\text{m}$ -thick polycrystalline foils (Johnson Matthey, 99.999% Cu, catalog #10950). The foils were annealed at 1000 °C for 45 min in atmospheric pressure Ar–H<sub>2</sub> in preparation for C deposition. Growth was performed in the chamber of a LEEM (base pressure  $\sim 1 \times 10^{-10}$  Torr), where the requisite C flux was generated from an electron-beam-heated graphite rod. The substrate temperature was monitored via a thermocouple welded to the sample mount. Foils were heated to 960 °C for 10 min and subsequently held at 840 °C for film growth. LEEM was used to continuously image the morphology of the sample surface throughout C deposition.

Post-growth analysis using selected-area LEED allowed the crystallography of the graphene domains to be correlated with their growth behavior. The relative orientation between the lattices of the graphene and Cu surface is the smallest angle observed between a first-order Cu diffraction spot and a first-order graphene diffraction spot (the  $C\langle 10 \rangle$  to  $Cu\langle 110 \rangle$  angle). This angle is  $\leq 15^\circ$ , by symmetry. Furthermore, by mapping the in-plane lattice orientation of individual

graphene domains onto their morphology we are able to examine the relationship between growth behavior and crystallography directly. This made it possible to identify the high-symmetry direction of the graphene lattice closest to the  $Cu\langle 100 \rangle$  direction along which the fast growth of that domain occurred.

## 3. Results

### 3.1. Anisotropic growth

We observed graphene to form polycrystalline, mostly 4-lobed islands on the Cu(001) surface. Each island lobe is a single graphene crystal, with its long axis (i.e., fast growth direction) roughly along a  $Cu\langle 100 \rangle$  in-plane direction (see Fig. 1a). If uninterrupted by surface irregularities, each graphene domain developed this morphology regardless of its lattice orientation.

Previous investigations of graphene growth on Cu(001) have shown how such four-lobed, polycrystalline islands may form. Multiple graphene domains nucleate near a common nucleation site. Four domains, whose in-plane orientations favor rapid growth, expand into elongated lobes at the expense of any less favorably oriented domains [4]. In the current paper we examine the relationship between the fast growth direction of graphene domains and their lattice orientation more closely and find that certain combinations of fast growth direction and lattice orientation occur much less frequently than others.

For a graphene domain approaching perfect alignment, i.e.,  $C(01)\parallel Cu\langle 110 \rangle$ , the fast growth direction is halfway between the two high-symmetry directions of the graphene lattice,  $C\langle 10 \rangle$  and  $C\langle 11 \rangle$  (see Fig. 2). The graphene edge perpendicular to the fast growth direction – that is, the “fast growth edge” where new carbon is being incorporated most rapidly – is similarly an equal blend of the armchair and zigzag edge configurations. The lattice rotation of a misaligned graphene domain moves the fast growth direction closer to either a  $C\langle 10 \rangle$  or  $C\langle 11 \rangle$  direction, with a corresponding shift in the edge structure (see Fig. 1b–e for examples of domains from each category). If fast growth is closer to a  $C\langle 11 \rangle$  direction the fast growth edge has a larger zigzag component, and domains growing fast along  $C\langle 10 \rangle$  have a larger armchair component in their fast growth edges. How the graphene lattice is oriented relative to the  $Cu\langle 100 \rangle$  in-plane direction thus dictates the structure of the graphene fast growth edge.

A summary of LEED data collected from over 130 different individual graphene domains shows the likelihood that the graphene lattice is rotated such that fast growth occurs closer to a  $C\langle 10 \rangle$  or  $C\langle 11 \rangle$  direction (Fig. 3). Of those graphene domains that are aligned within  $\pm 3^\circ$  of the Cu surface, approximately an equal number are rotated in either direction. When the lattice misalignment increases to  $\pm 3$ – $6^\circ$  or  $\pm 6$ – $9^\circ$ ,  $\sim 60\%$  of domains are oriented such that fast growth occurs closer to a  $C\langle 10 \rangle$  direction. The distribution increasingly favors the  $C\langle 10 \rangle$  directions for larger lattice rotations. For instance, approximately 70% of domains misaligned by  $\pm 9$ – $12^\circ$  are rotated such that a  $C\langle 10 \rangle$  direction is closer to the fast growth direction. This proportion jumps to  $\sim 90\%$

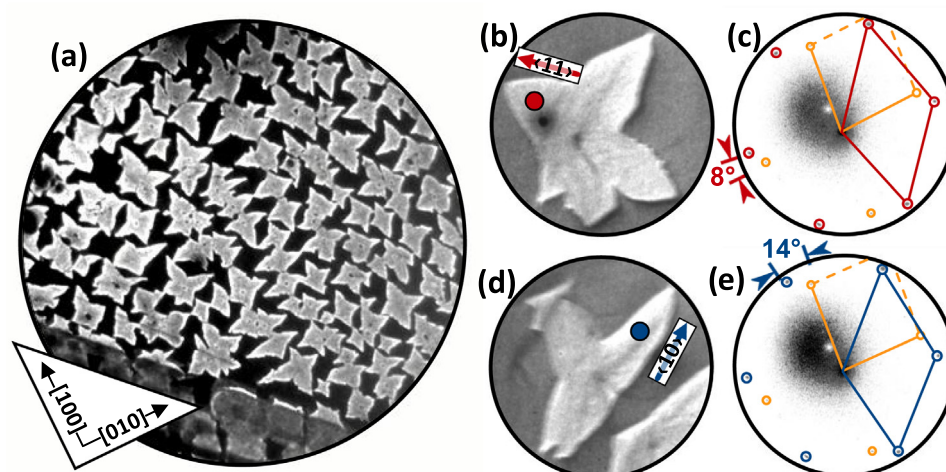


**Fig. 1** – LEEM micrographs (a, b and d) and LEED patterns (c and e) examining graphene domains on Cu(001). The red and blue dots in (b) and (d) are the locations where (c) and (e) were collected, respectively. The orange (red, blue) circles in (c) and (e) are centered on Cu (graphene) diffraction spots. The reciprocal unit cells of the graphene (red, blue) and Cu surface (orange) are shown in (c and e). Many graphene islands growing on Cu(001) develop a distinct 4-lobed morphology, where the long axes of the lobes lie close to a Cu(100) in-plane direction, as is shown by the consistent island-to-island orientation in (a) [Field of view (FOV) = 46  $\mu\text{m}$ ]. Also in (a) are graphene islands of other shapes, which typically form due to interactions with surface inhomogeneities or other graphene islands. The dark lower-left portion of (a) is a twinned region of the Cu(001) substrate. The lattice of the graphene domain in (b and c) is rotated 8° from Cu(110) (see spacer-arrows) in such a way that a C(11) direction [red arrow in (b)] is closer to the Cu(100) direction along which fast growth occurred. In contrast, the 14° lattice rotation (spacer-arrows) of the domain in (d and e) resulted in the Cu(100) fast growth direction being near a C(10) lattice direction [blue arrow in (d)]. FOV in (b and d) is 7  $\mu\text{m}$ . (A color version of this figure can be viewed online.)

for the domains rotated by  $\pm 12\text{--}15^\circ$ , which means that nearly all these domains have their fast growth directions very close to a C(10) direction. Correspondingly, the graphene edge at the tips of these fast-growing lobes has the armchair configuration (see Fig. 2). The relative absence of graphene domains with fast growth occurring along a C(11) direction implies that carbon incorporation becomes increasingly unfavorable as the graphene edge approaches the purely zigzag configuration.

When a fast growth direction was close to a C(11) lattice direction we found that the domain tended to be part of a polycrystalline graphene island with an atypical domain structure. The domain distribution of a typical four-lobed island is for each lobe to be a discrete graphene crystal differentiated from the island's other constituent domains by its particular lattice orientation – the “domain-lobes” thus being separated by rotational grain boundaries. However, in these unusual islands two neighboring lobes have precisely the same lattice orientation, reflecting that they are instead part of a single graphene domain that includes both lobes (see outlined region in Fig. 4b). The over-all four-lobed island morphology is preserved despite this atypical domain distribution, including the restriction of graphene fast growth to the (100) in-plane directions of the Cu substrate. This combination of island morphology and crystallographic configuration dictates that one lobe of the multi-lobe domain undergoes fast growth closer to a C(10) direction (blue outlined lobe in Fig. 4b) while the other lobe is C(11)-oriented (red outlined lobe in Fig. 4b). A possible reason for this behavior is that there was no suitable graphene nucleus to expand

into the forth “domain-lobe” of these atypical islands. This absence may have allowed the neighboring “domain-lobe” to undergo fast growth along the second, perpendicular Cu(100) direction despite the C(11)-oriented growth configuration. If true, this scenario suggests that fast growth along the C(11) directions may be even less favorable than the distribution of orientations reported in Fig. 3 indicates.

### 3.2. The graphene–Cu(001) moiré

Rotating the graphene lattice also changes the moiré it forms with the Cu surface. Selected-area LEED patterns collected from graphene domains within  $\pm 9^\circ$  of alignment with the Cu(001) substrate (i.e., C(01) || Cu(110)) often have two diffraction spots in addition to those directly attributable to the C and Cu lattices (Fig. 5). These extra spots are not observed when the lattice misalignment is larger than  $\sim \pm 9^\circ$ . The orientation and separation of these diffraction spots vary, and when calibrated with the graphene and Cu patterns suggest a physical structure with a periodicity ranging from 8.4 to 12.3 Å. Scanning-tunneling microscopy studies of graphene on Cu(001) have reported the ridged moiré to have periodicities of 11 Å [12],  $12 \pm 1$  Å [13], and 13.5 Å [14], which generally agree with the range seen here. Thus, we attribute the additional diffraction spots to the graphene–Cu(001) moiré.

To ascertain how the graphene–Cu(001) moiré evolves as the orientation between the two materials changes, LEED from graphene domains with many different orientations was analyzed, as is summarized in Fig. 6. The LEED patterns examined include the full range of graphene orientations

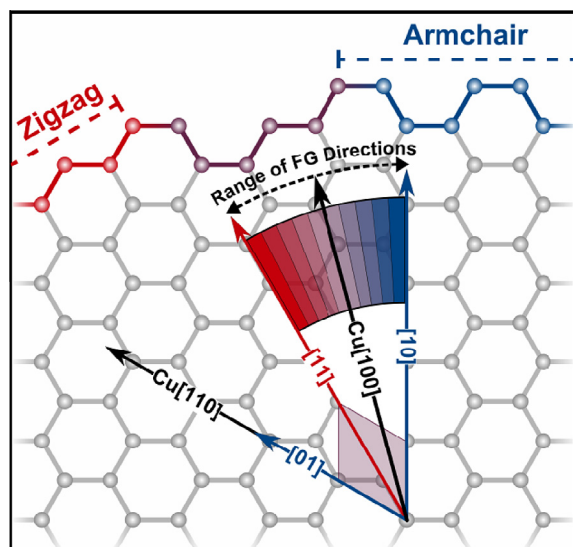


Fig. 2 – Schematic diagram illustrating lattice directions and edges of the graphene lattice (the purple diamond is the graphene unit cell). Because the fast growth direction remains near a Cu<100> direction, a rotation of the graphene lattice changes the lattice direction along which fast growth occurs. When the lattice of a graphene domain approaches perfect alignment with the Cu(001) surface (i.e.,  $C[01] \parallel Cu[110]$  or  $Cu[1\bar{1}0]$ , see arrows on left of unit cell) the fast growth direction is directly between a C<10> and a C<11> direction. Any rotation away from alignment moves the fast growth direction toward either the C<10> or C<11> direction. A graphene edge that is perpendicular to a C<10> direction (blue) has the armchair structure, while an edge perpendicular to a C<11> direction (red) has the zigzag structure. The purple edge section is a mix of these two high-symmetry edge structures. (A color version of this figure can be viewed online.)

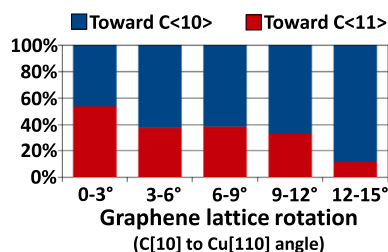


Fig. 3 – The proportion of graphene domains with their fast growth direction toward a C<10> or C<11> lattice direction, as a function of the graphene rotation angle. For small rotations, fast growth is equally likely to be toward a C<11> or C<10> direction. However, the majority of graphene domains that are misaligned relative to the Cu(001) surface by more than 9° undergo fast growth near a C<10> lattice direction. (A color version of this figure can be viewed online.)

with observable moiré diffraction spots, covering a  $\sim 18^\circ$  arc centered on the perfectly aligned configuration. As the graphene lattice swivels from  $+9^\circ$  to  $-9^\circ$  the orientation of the

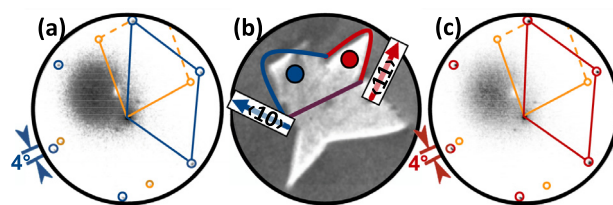


Fig. 4 – LEED patterns (a and c) and a LEEM micrograph (b) examining a graphene island on Cu(001). The blue and red dots in (b) are where (a) and (c) were collected, respectively. The orange (red, blue) circles in (c) and (e) are centered on Cu (graphene) diffraction spots. The reciprocal unit cells of the graphene (red, blue) and Cu surface (orange) are shown in (a) and (c). Occasionally graphene islands have an atypical domain structure, where two neighboring island lobes are part of a single domain [see approximate domain outline in (b)]. In these circumstances, the Cu<100> direction along which one lobe (blue outline) grew is closer to a C<10> direction (blue arrow) making it armchair-oriented, while its neighbor (red outline) has a C<11> direction (red arrow) closer to its Cu<100> fast growth direction leading it to be zigzag-tipped. Coincidental Cu step-edge clustering (dark ribbon above blue-outlined lobe) has distorted the C<10>-oriented lobe (blue), preventing it from developing a smooth perimeter. The lattice rotation of the graphene domain is  $4^\circ$ , and the FOV in (b) is  $7 \mu\text{m}$ . (A color version of this figure can be viewed online.)

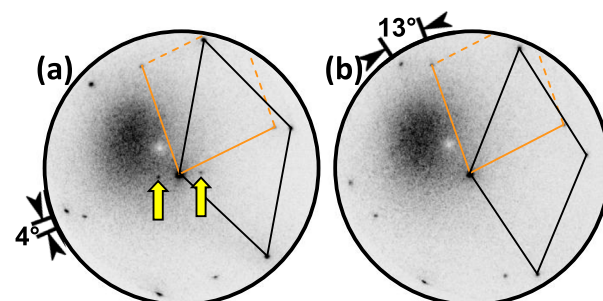
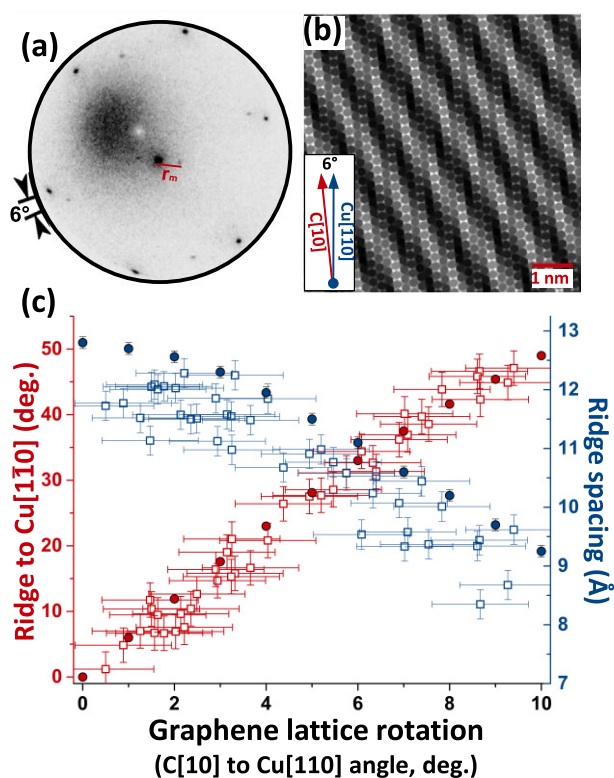


Fig. 5 – LEED patterns from graphene domains grown on Cu(001). The reciprocal unit cells of the graphene (black) and Cu surface (orange) are shown. Diffraction spots from the ridged graphene–Cu(001) moiré can be seen in (a) (yellow arrows, lattice rotation is  $4^\circ$ ). Diffraction from domains rotated by more than  $\sim 9^\circ$ , such as (b), does not show evidence of the ridged moiré (lattice rotation is  $13^\circ$ ). The orientation and periodicity of the moiré ridges change with the graphene lattice orientation. (A color version of this figure can be viewed online.)

two moiré diffraction spots rotates by  $\sim 90^\circ$ , starting nearly parallel to Cu[010], moving through Cu[110] when the graphene lattice is perfectly aligned ( $0^\circ$ ), and ending with the ridges roughly parallel to Cu[100] ( $-9^\circ$ ). The periodicity of the ridges varies simultaneously, with the shortest wavelength of  $8.4 \text{ \AA}$  when the moiré is parallel to a Cu<100> direction, and the longest of  $12.3 \text{ \AA}$  when it is parallel to a Cu<110>





**Fig. 6** – LEED from a graphene domain grown on Cu(001) (a) showing the diffraction spots of the ridged graphene–Cu(001) moiré (graphene lattice rotation is  $6^\circ$ ). (b) A rendering from a simple geometric model of the graphene–Cu(001) surface, with the graphene lattice rotated by  $6^\circ$  (please see Ref. [15] for model details). Brighter C atoms are higher. The ridged moiré is clearly visible. (c) Orientation and periodicity of the graphene–Cu(001) moiré vs. graphene rotation. Open squares are experiment. Filled circles result from an atomic model. (A color version of this figure can be viewed online.)

direction. For a perfectly aligned graphene domain, the ridges are along a zigzag direction; for misalignments of  $\sim 7^\circ$  the ridges are rotated  $\sim 37^\circ$  with respect to Cu[110] and thus nearly parallel to an armchair direction.

To determine if the observed orientations and periodicities of the moiré are purely the result of geometry, we compare them with an atomic simulation of laterally unstrained graphene and Cu(001) lattices based on simple geometric rules. As Fig. 6c shows, the orientation of the moiré ridges is accurately reproduced (please see Ref. [15] for simulation details). However, the ridge spacing observed by LEED is slightly smaller than predicted by the model. The discrepancy is likely the result of a small dilation in the LEED patterns near the specular beam. This would introduce systemic error to the measured ridge spacing while preserving angular fidelity, thus not altering the observed ridge orientation. The excellent agreement between observation and model suggest that the details of the ridged graphene–Cu(001) moiré are a straightforward result of the geometry of the two lattices.

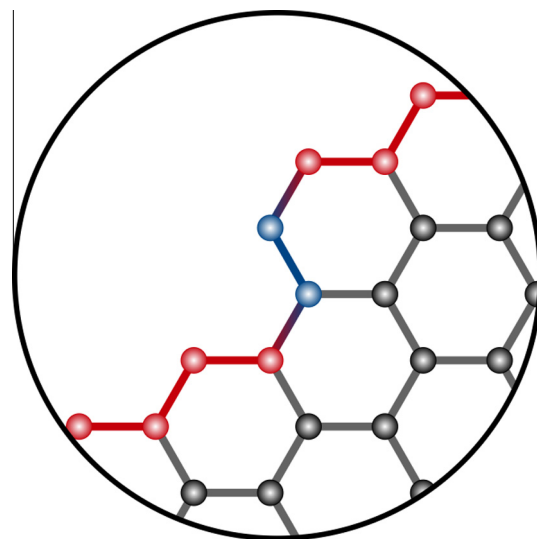


**Fig. 7** – A schematic diagram of an armchair-step, or kink (blue), in a majority-zigzag graphene edge (red). Such kinks may facilitate adatom attachment during graphene growth on Cu(001). (A color version of this figure can be viewed online.)

#### 4. Discussion

We have observed that although graphene on Cu(001) undergoes attachment-limited, anisotropic growth regardless of its lattice orientation, certain graphene orientations occur less often than others. Only a small fraction of fast growth directions are close to a C[11] direction, which suggests carbon adatom incorporation at zigzag graphene edges is unfavorable. By further examining the observed distribution of graphene orientations in the context of attachment-limited growth we are able to gain additional insight into the relationship between graphene lattice orientation and growth behavior. As on many metal surfaces, graphene growth on Cu(001) is an attachment-limited process, meaning that the incorporation of carbon adatoms at the edge of the graphene sheet is the rate-limiting step in the expansion of the graphene crystal [4,16–18]. Thus, the specific atomic geometry at the growth front provides insight into the atomic nature of the growth. For instance, the attachment-limited growth of graphene on Ru(0001) and Ir(111) is mediated by the incorporation of multi-atom carbon clusters at majority zigzag edges. Each cluster attachment event creates two kinks in the zigzag edge, which then act as attachment sites for further carbon adatom incorporation (see Fig. 7) [16,19]. Similarly, CVD experiments on Pt foil substrates have shown a strong correlation between the line-density of kinks in zigzag graphene edges and their growth and etching rates [20]. The increased likelihood of accelerated growth occurring along the C[10] directions is consistent with the armchair edge structure serving a similar function in graphene growth on Cu(001). Conversely, as the graphene edge approaches a purely zigzag structure there are fewer available adatom attachment sites and growth is inhibited. The kink-mediated adatom attachment process suggested by this interpretation

is consistent with recent simulations of graphene growth on Cu(001), and other metals [21,22].

We may also look to ambient-pressure CVD and seeded graphene growth on Cu(001) for insight into the role of kinks in mediating adatom attachment. This growth process can yield hexagonal, single-domain islands that are bound by zigzag edges [23]. Because kinetically determined crystal shapes are typically terminated by their slowest growing facets [24], this supports the conclusion that carbon attachment is inhibited at purely zigzag graphene edges. We emphasize that regardless of the graphene lattice orientation it is the Cu surface that dictates the possible fast growth directions. The significance of Cu surface structure for graphene growth behavior is further illustrated by a recent study showing hybridization between zigzag edge states with Cu atoms along the  $\langle 101 \rangle$  directions of Cu(001) and (101) [25]. So, while kink-mediated adatom attachment is consistent with the observed growth behavior, it is only part of a more complex explanation.

The ridged moiré formed by graphene may also factor into its attachment-limited, anisotropic growth mode on Cu(001), although this is unlikely. A rotation of the graphene lattice such that C[10] is closer to the fast growth direction causes the moiré ridges to simultaneously rotate away from the fast growth direction, eventually becoming perpendicular once the graphene lattice is rotated by  $\sim 9^\circ$ . The opposite is true for rotations toward C[11], with the ridges eventually becoming parallel to the fast growth direction. If the moiré ridges persist to the perimeter of the graphene sheet they would further differentiate the atomic geometry at the growth front. However, the moiré pattern was only detected in graphene domains within  $\pm 9^\circ$  of alignment with the Cu surface, where an approximately equal number of domains are rotated toward the C(10) and C(11) directions. This evidence supports the conclusion that it is the change in edge structure caused by a lattice rotation, and not the associated change in the moiré pattern, which reduces the likelihood for accelerated growth along the C(11) directions.

## 5. Summary

In summary, we have used LEEM and LEED to examine how the growth and structure of graphene on Cu(001) are affected by the relative orientation of the two lattices. The superposition of the hexagonal graphene lattice on the (001) Cu surface results in a ridged moiré, where the orientation and spacing of the ridges depend on the relative graphene orientation. The orientation of the graphene lattice also determines the structure of the graphene edge perpendicular to the Cu(100), fast growth direction. Rarely do we find graphene domains with fast growth occurring close to a C(11) direction, suggesting that adatom incorporation is mediated by kinks, and is thus less likely at purely zigzag graphene edges. Although this interpretation is consistent with the relevant literature, it does not elucidate the mechanism through which fast growth is restricted to the Cu(100) in-plane directions. Identifying the importance of kinks in the attachment limited growth of graphene on Cu(001) is none-the-less an

important step in harnessing the technological potential of this growth method.

## Acknowledgments

This work was supported by the NSF under Grant No. DMR-1105541 (ODD and JMW) and by the Director, Office of Science, Office of Basic Energy Sciences, Division of Materials Sciences and Engineering, of the U.S. Department of Energy Contract No. De-Ac04-94AL85000 (SN, KT, and KFM).

## REFERENCES

- [1] Li X, Cai W, An J, Kim S, Nah J, Yang D, et al. Large-area synthesis of high-quality and uniform graphene films on copper foils. *Science* 2009;324:1312–4. <http://dx.doi.org/10.1126/science.1171245>.
- [2] Li X, Cai W, Colombo L, Ruoff RS. Evolution of graphene growth on Ni and Cu by carbon isotope labeling. *Nano Lett* 2009;9:4268–72. <http://dx.doi.org/10.1021/nl902515k>.
- [3] Bae S, Kim H, Lee Y, Xu X, Park J-S, Zheng Y, et al. Roll-to-roll production of 30-inch graphene films for transparent electrodes. *Nat Nanotechnol* 2010;5:574–8.
- [4] Wofford JM, Nie S, McCarty KF, Bartelt NC, Dubon OD. Graphene islands on Cu foils: the interplay between shape, orientation, and defects. *Nano Lett* 2010;10:4890–6. <http://dx.doi.org/10.1021/nl102788f>.
- [5] Li X, Magnuson CW, Venuopal A, Tromp RM, Hannon JB, Vogel EM, et al. Large-area graphene single crystals grown by low-pressure chemical vapor deposition of methane on copper. *J Am Chem Soc* 2011;133:2816–9. <http://dx.doi.org/10.1021/ja109793s>.
- [6] Chen S, Ji H, Chou H, Li Q, Li H, Suk JW, et al. Millimeter-size single-crystal graphene by suppressing evaporative loss of Cu during low pressure chemical vapor deposition. *Adv Mater* 2013;25:2062–5. <http://dx.doi.org/10.1002/adma.201204000>.
- [7] N'Diaye A, Bleikamp S, Feibelman P, Michely T. Two-dimensional Ir cluster lattice on a graphene moiré on Ir (111). *Phys Rev Lett* 2006;97:215501. <http://dx.doi.org/10.1103/PhysRevLett.97.215501>.
- [8] Marchini S, Günther S, Wintterlin J. Scanning tunneling microscopy of graphene on Ru (0001). *Phys Rev B* 2007;76:075429. <http://dx.doi.org/10.1103/PhysRevB.76.075429>.
- [9] Gao L, Guest JR, Guisinger NP. Epitaxial graphene on Cu(111). *Nano Lett* 2010;10:3512–6. <http://dx.doi.org/10.1021/nl1016706>.
- [10] Murata Y, Petrova V, Kappes BB, Ebnonnasir A, Petrov I, Xie Y-H, et al. Moiré superstructures of graphene on faceted Nickel islands. *ACS Nano* 2010;4:6509–14. <http://dx.doi.org/10.1021/nn102446y>.
- [11] Nie S, Bartelt NC, Wofford JM, Dubon OD, McCarty KF, Thürmer K. Scanning tunneling microscopy study of graphene on Au (111): growth mechanisms and substrate interactions. *Phys Rev B* 2012;85:205406. <http://dx.doi.org/10.1103/PhysRevB.85.205406>.
- [12] Zhao L, Rim KT, Zhou H, He R, Heinz TF, Pinczuk A, et al. Influence of copper crystal surface on the CVD growth of large area monolayer graphene. *Solid State Commun* 2011;151:509–13. <http://dx.doi.org/10.1016/j.ssc.2011.01.014>.
- [13] Cho J, Gao L, Tian J, Cao H, Wu W, Yu Q, et al. Atomic-scale investigation of graphene grown on Cu foil and the effects of thermal annealing. *ACS Nano* 2011;5:3607–13.

- [14] Rasool HI, Song EB, Mecklenburg M, Regan BC, Wang KL, Weiller BH, et al. Atomic-scale characterization of graphene grown on copper (100) single crystals. *J Am Chem Soc* 2011;133:12536–43.
- [15] Wofford JM, Starodub E, Walter AL, Nie S, Bostwick A, Bartelt NC, et al. Extraordinary epitaxial alignment of graphene islands on Au (111). *New J Phys* 2012;14:053008. <http://dx.doi.org/10.1088/1367-2630/14/5/053008>.
- [16] Loginova E, Bartelt NC, Feibelman PJ, McCarty KF. Evidence for graphene growth by C cluster attachment. *New J Phys* 2008;10:93026. <http://dx.doi.org/10.1088/1367-2630/10/9/093026>.
- [17] McCarty KF, Feibelman PJ, Loginova E, Bartelt NC. Kinetics and thermodynamics of carbon segregation and graphene growth on Ru (0001). *Carbon* 2009;47:1806–13. <http://dx.doi.org/10.1016/j.carbon.2009.03.004>.
- [18] Loginova E, Bartelt NC, Feibelman PJ, McCarty KF. Factors influencing graphene growth on metal surfaces. *New J Phys* 2009;11:063046. <http://dx.doi.org/10.1088/1367-2630/11/6/063046>.
- [19] Rogge PC, Nie S, McCarty KF, Bartelt NC, Dubon OD. Orientation-dependent growth mechanisms of graphene islands on Ir (111). *Nano Lett* 2015;15:170–5. <http://dx.doi.org/10.1021/nl503340h>.
- [20] Ma T, Ren W, Zhang X, Liu Z, Gao Y, Yin L, et al. Edge-controlled growth and kinetics of single-crystal graphene domains by chemical vapor deposition. *Proc Natl Acad Sci USA* 2013;110:20386–91. <http://dx.doi.org/10.1073/pnas.1312802110>.
- [21] Luo Z, Kim S, Kawamoto N, Rappe AM, Johnson ATC. Growth mechanism of hexagonal-shape graphene flakes with zigzag edges. *ACS Nano* 2011;5:9154–60. <http://dx.doi.org/10.1021/nn203381k>.
- [22] Artyukhov VI, Liu Y, Yakobson BI. Equilibrium at the edge and atomistic mechanisms of graphene growth. *Proc Natl Acad Sci USA* 2012;109:15136–40. <http://dx.doi.org/10.1073/pnas.1207519109>.
- [23] Yu Q, Jauregui La, Wu W, Colby R, Tian J, Su Z, et al. Control and characterization of individual grains and grain boundaries in graphene grown by chemical vapour deposition. *Nat Mater* 2011;10:443–9. <http://dx.doi.org/10.1038/nmat3010>.
- [24] Frank F. In: Doremus R, Roberts B, Turnbull D, editors. *Proc Int Conf Cryst Growth*. New York: Wiley; 1958. p. 411.
- [25] Murdock AT, Koos A, Ben BT, Houben L, Batten T, Zhang T, et al. Controlling the orientation, edge geometry, and thickness of chemical vapor deposition graphene. *ACS Nano* 2013;7:1351–9. <http://dx.doi.org/10.1021/nn3049297>.